New Coplanar $(ABA)_n$-Type Donor−Acceptor π-Conjugated Copolymers Constituted of Alkylthiophene (Unit A) and Pyridazine (Unit B): Synthesis Using Hexamethylditin, Self-Organized Solid Structure, and Optical and Electrochemical Properties of the Copolymers

Takuma Yasuda,[†] Yoshimasa Sakai,[‡] Shinji Aramaki,[‡] and Takakazu Yamamoto*,[†]

Chemical Resources Laboratory, Tokyo Institute of Technology, 4259 Nagatsuta, Midori-ku, Yokohama 226-8503, Japan, and Mitsubishi Chemical Group Science and Technology Research Center, Inc., 1000 Kamoshida-cho, Aoba-ku, Yokohama 227-8502, Japan

Received July 18, 2005. Revised Manuscript Received September 20, 2005

A new series of π-conjugated $(ABA)_n$-type polymers constructed of electron-donating thiophene or 3-alkylthiophene (as the unit A) and electron-accepting pyridazine (as the unit B) were synthesized via palladium-catalyzed dehalogenative polycondensation of Br−ABA−Br using hexamethylditin as the condensing reagent. The obtained polymers were characterized by NMR, IR, and elemental analysis. The polymers with alkyl side chains were soluble in organic solvents, and gave number-average molecular weights ranging from 3.2×10^4 to 16×10^4 in gel-permeation analysis. The polymers exhibited strong green photoluminescence (PL) with the peak in the range of 510−520 nm and quantum yields of 51−61% in chloroform. The PL intensity was sensitive toward acids. In films, the UV−vis and PL peaks shifted to a longer wavelength by about 30−40 nm. Powder X-ray diffraction data suggested that the polymer formed a highly ordered π-stacked assembly assisted by the side chain crystallization and dipole−dipole interaction. Cyclic voltammetry revealed that the polymer was susceptible to both electrochemical p- and n-doping, and the n-doping peak appeared in the range of −2.15 to −2.28 V vs Ag^+/Ag. The polymer served as a good material for a thin-film field-effect transistor and gave a hole mobility of 3×10^{-3} cm^2 V^{-1} s^{-1}.

Introduction

Polythiophenes occupy a prominent position of research in π-conjugated polymers because of their attractive electronic and optical properties.[1] In particular, chemical and physical properties of regioregular head-to-tail poly(3-alkylthiophene-2,5-diyl)s (HT-P3RTh's)[2−6] have widely been studied. They show excellent performance in organic electronic devices such as thin-film field-effect transistors (FETs)[5] and photovoltaic cells.[6] HT-P3RTh forms a well-ordered lamellar structure with strong cofacial π-stacking in the solid state, which is a desirable feature to attain a high charge carrier mobility in FETs.[5]

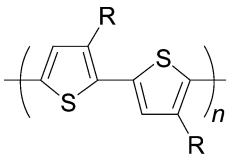

HT-P3RTh[2-6]

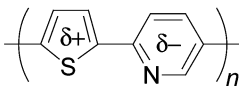

PThPy[7]

To tune the electronic properties of polythiophenes and to create new self-assembling supramolecular structures, π-conjugated copolymers of thiophene with electron-deficient azaheterocycles (e.g., pyridine to produce the above shown PThPy,[7] quinoxaline,[7a,8] thiazole,[9] 1,2,4-triazole,[10a] and 1,3,4-thiadiazole[10]) have been prepared and their chemical and physical properties have been investigated. These copolymers

* To whom correspondence should be addressed. E-mail: tyamamot@res.titech.ac.jp.

[†] Tokyo Institute of Technology.

[‡] Mitsubishi Chemical Group Science and Technology Research Center, Inc.

(1) (a) McCullough, R. D. *Adv. Mater.* **1998**, *10*, 93. (b) Leclerc, M.; Faid, K. *Adv. Mater.* **1997**, *9*, 1087. (c) Roncali, J. *Chem. Rev.* **1992**, *92*, 711. (d) Schopf, G.; Kossmehl, G. *Adv. Polym. Sci.* **1997**, *129*, 1. (e) Yamamoto, T. *Synlett* **2003**, 425.

(2) (a) McCullough, R. D.; Lowe, R. D.; Jayaraman, M.; Anderson, D. L. *J. Org. Chem.* **1993**, *58*, 904. (b) McCullough, R. D.; Tristram-Nagle, S.; Williams, S. P.; Lowe, R. D.; Jayaraman, M. *J. Am. Chem. Soc.* **1993**, *115*, 4910.

(3) Chen, T.-A.; Wu, X.; Rieke, R. D. *J. Am. Chem. Soc.* **1995**, *117*, 233.

(4) Yamamoto, T.; Komarudin, D.; Arai, M.; Lee, B.-L.; Suganuma, H.; Asakawa, N.; Inoue, Y.; Kubota, K.; Sasaki, S.; Fukuda, T.; Matsuda, H. *J. Am. Chem. Soc.* **1998**, *120*, 2047.

(5) (a) Sirringhaus, H.; Tessler, N.; Friend, R. H. *Science* **1998**, *280*, 1741. (b) Bao, Z.; Dodabalapur, A.; Lovinger, A. J. *Appl. Phys. Lett.* **1996**, *69*, 4108. (c) Sirringhaus, H.; Brown, P. J.; Friend, R. H.; Nielsen, M. M.; Bechgaard, K.; Langeveld-Voss, B. M. W.; Spiering, A. J. H.; Janssen, R. A. J.; Meijer, E. W.; Herwig, P.; de Leeuw, D. M. *Nature* **1999**, *401*, 685.

(6) (a) Huynh, W. U.; Dittmer, J. J.; Alivisatos, A. P. *Science* **2002**, *295*, 2425. (b) Dittmer, J. J.; Marseglia, E. A.; Friend, R. H. *Adv. Mater.* **2000**, *12*, 1270.

(7) (a) Yamamoto, T.; Zhou, Z.-H.; Kanbara, T.; Shimura, M.; Kizu, K.; Maruyama, T.; Nakamura, Y.; Fukuda, T.; Lee, B.-L.; Ooba, N.; Tomaru, S.; Kurihara, T.; Kaino, T.; Kubota, K.; Sasaki, S. *J. Am. Chem. Soc.* **1996**, *118*, 10389. (b) Zhou, Z.-H.; Maruyama, T.; Kanbara, T.; Ikeda, T.; Ichimura, K.; Yamamoto, T.; Tokuda, K. *J. Chem. Soc., Chem. Commun.* **1991**, 1210.

(8) (a) Kanbara, T.; Miyazaki, Y.; Yamamoto, T. *J. Polym. Sci., Part A: Polym. Chem.* **1995**, *33*, 999. (b) Yamamoto, T.; Lee, B.-L.; Kokubo, H.; Kishida, H.; Hirota, K.; Wakabayashi, T.; Okamoto, H. *Macromol. Rapid Commun.* **2003**, *24*, 440.

10.1021/cm051561y CCC: $30.25
Published on Web 11/01/2005

Chart 1. Reported Thiophene-Based (ABA)$_n$-Type Copolymer and New Copolymer of Pyridazine, P(PydTh)

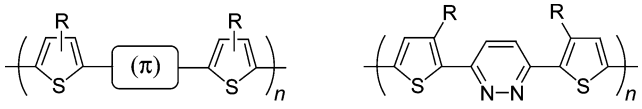

P(PydTh)

composed of the alternating sequence of electron-donating and electron-accepting aromatic units exhibit interesting electronic and optical properties such as large optical third-order nonlinearity[7a,8b] based on their intramolecular charge-transferred (CT) electronic structure.

Another family of thiophene-based π-conjugated copolymers with the above shown (ABA)$_n$-type structure has also been attracting intensive attentions.[11−17] For the (π) unit in Chart 1, various *p*-phenylene-based[12a−c,13c,14c,15,17a,d] and thiophene-based[11,13a,14a,c,15,16] units have been employed. However, use of electron-accepting azaheterocycles as the (π) unit has received less attention.[12d,14b,17c]

Pyridazine is one of the strongest electron-accepting azaheterocycles because of its containing two electron-withdrawing imine −C═N− nitrogens.[18] In this study, we focus on synthesis and chemical properties of new thiophene-based (ABA)$_n$-type π-conjugated copolymers with the electron-deficient pyridazine unit as the B or the (π) unit. The CT electronic structure and symmetrical structure of the obtained copolymers, **P(PydTh)s**, as well as known S···N interactions[19] may lead to unique molecular assembly of the polymer. Pyridazines have been studied as a metal-coordinating ligand[20] and a component for supramolecular architectures.[21] However, to our knowledge, π-conjugated copolymer bearing the pyridazine unit has no precedent. Herein, we report results of synthesis of the new (ABA)$_n$-type π-conjugated polymers and their chemical properties including self-assembling character. For the synthesis of the polymer, a new route using hexamethylditin ($Me_3Sn-SnMe_3$) as a condensing reagent has been designed.

Scheme 1

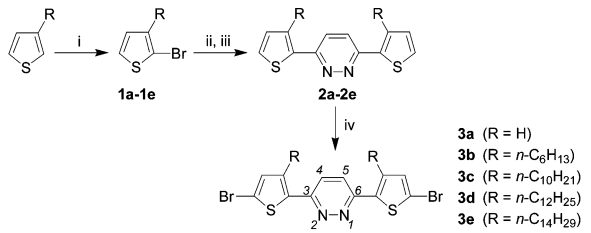

(i) NBS (1 equiv.), DMF, room temperature; (ii) Mg, THF, 60 °C; (iii) 3,6-dichloropyridazine, $NiCl_2$(dppp) (dppp = 1,3-bis(diphenylphosphino)propane), THF, 60 °C; (iv) NBS (2 equiv.), DMF, 60 °C.

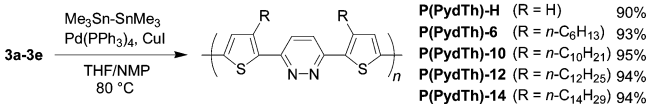

Results and Discussion

Synthesis of Monomers and Polymers. Syntheses of the dibromo monomers (**3a**−**3e**) and the corresponding polymers are outlined in Scheme 1. The key in the polymerization is a new synthetic methodology using hexamethylditin ($Me_3Sn-SnMe_3$) as the condensing reagent in the presence of Pd catalyst.

Bromination of 3-alkylthiophene (step i in Scheme 1) was achieved by using *N*-bromosuccinimide (NBS) in DMF.[22] The coupling reaction between 3,6-dichloropyridazine and the Grignard reagent of **1a**−**1e** in the presence of a catalytic amount of $NiCl_2$(dppp) afforded trimeric compounds (**2a**−**2e**) in 58−74% yields. **2a**−**2e** were brominated by NBS to give the corresponding dibromo monomers (**3a**−**3e**). The structure of **3a**−**3e** was ascertained by ^{1}H NMR, ^{13}C NMR,

(9) (a) Yamamoto, T.; Arai, M.; Kokubo, H.; Sasaki, S. *Macromolecules* **2003**, *36*, 7986. (b) Yamamoto, T.; Arai, M.; Kokubo, H.; Sasaki, S. *J. Polym. Sci., Part A: Polym. Chem.* **2003**, *41*, 1449. (c) Yamamoto, T.; Kokubo, H.; Kobashi, M.; Sakai, Y. *Chem. Mater.* **2004**, *16*, 4616.
(10) (a) Yasuda, T.; Imase, T.; Sasaki, S.; Yamamoto, T. *Macromolecules* **2005**, *38*, 1500. (b) Yamamoto, T.; Yasuda, T.; Sakai, Y.; Aramaki, S. *Macromol. Rapid Commun.* **2005**, *26*, 1214.
(11) (a) Wu, Y.; Liu, P.; Gardner, S.; Ong, B. S. *Chem. Mater.* **2005**, *17*, 221. (b) Ong, B. S.; Wu, Y.; Liu, P.; Gardner, S. *J. Am. Chem. Soc.* **2004**, *126*, 3378. (c) Heeney, M.; Bailey, C.; Genevicius, K.; Shkunov, M.; Sparrowe, D.; Tierney, S.; McCulloch, I. *J. Am. Chem. Soc.* **2005**, *127*, 1078. (d) McCulloch, I.; Bailey, C.; Giles, M.; Heeney, M.; Love, I.; Shkunov, M.; Sparrowe, D.; Tierney, S. *Chem. Mater.* **2005**, *17*, 1381.
(12) (a) Reynolds, J. R.; Ruiz, J. P.; Child, A. D.; Nayak, K.; Marynick, D. S. *Macromolecules* **1991**, *24*, 678. (b) Ruiz, J. P.; Dharia, J. R.; Reynolds, J. R.; Buckley, L. J. *Macromolecules* **1992**, *25*, 849. (c) Argun, A. A.; Cirpan, A.; Reynolds, J. R. *Adv. Mater.* **2003**, *15*, 1338. (d) DuBois, C. J.; Abboud, K. A.; Reynolds, J. R. *J. Phys. Chem. B* **2004**, *108*, 8550.
(13) (a) Sonmez, G.; Shen, C. K. F.; Rubin, Y.; Wudl, F. *Angew. Chem., Int. Ed.* **2004**, *43*, 1498. (b) Sonmez, G.; Sonmez, H. B.; Shen, C. K. F.; Jost, R. W.; Rubin, Y.; Wudl, F. *Macromolecules* **2005**, *38*, 669. (c) Sonmez, G.; Meng, H.; Wudl, F. *Chem. Mater.* **2004**, *16*, 574.
(14) (a) Ng, S. C.; Xu, J. M.; Chan, H. S. O. *Macromolecules* **2000**, *33*, 7349. (b) Lu, H.-F.; Chan, H. S. O.; Ng, S.-C. *Macromolecules* **2003**, *36*, 1543. (c) Xu, J.; Ng, S. C.; Chan, H. S. O. *Bull. Chem. Soc. Jpn.* **2003**, *76*, 1449.
(15) (a) Kitamura, C.; Tanaka, S.; Yamashita, Y. *Chem. Mater.* **1996**, *8*, 570. (b) Karikomi, M.; Kitamura, C.; Tanaka, S.; Yamashita, Y. *J. Am. Chem. Soc.* **1995**, *117*, 6791. (c) Kitamura, C.; Tanaka, S.; Yamashita, Y. *J. Chem. Soc., Chem. Commun.* **1994**, 1585.
(16) (a) Kokubo, H.; Yamamoto, T. *Macromol. Chem. Phys.* **2001**, *202*, 1031. (b) Gallazzi, M. C.; Castellani, L.; Marin, R. A.; Zerbi, G. *J. Polym. Sci., Part A: Polym. Chem.* **1993**, *31*, 3339. (c) Mårdalen, J.; Fell, H. J.; Samuelsen, E. J.; Bakken, E.; Carlsen, P. H. J.; Andersson, M. R. *Macromol. Chem. Phys.* **1995**, *196*, 553.
(17) (a) Danieli, R.; Ostoja, P.; Tiecco, M.; Zamboni, R.; Taliani, C. *J. Chem. Soc., Chem. Commun.* **1986**, 1473. (b) Jenkins, I. H.; Salzner, U.; Pickup, P. G. *Chem. Mater.* **1996**, *8*, 2444. (c) Liu, B.; Yu, W.-L.; Lai, Y.-H.; Huang, W. *Macromolecules* **2000**, *33*, 8945. (d) Pei, J.; Yu, W.-L.; Ni, J.; Lai, Y.-H.; Huang, W.; Heeger, A. J. *Macromolecules* **2001**, *34*, 7241. (e) Wang, F.; Lai, Y.-H. *Macromolecules* **2003**, *36*, 536. (f) Jayakannan, M.; van Hal, P. A.; Janssen, R. A. J. *J. Polym. Sci., Part A: Polym. Chem.* **2001**, *40*, 251.
(18) (a) Nenner, I.; Schulz, G. J. *J. Chem. Phys.* **1975**, *62*, 1747. (b) Tabner, B. J.; Yandle, J. R. *J. Chem. Soc. (A)* **1968**, 381.
(19) (a) Iwasaki, F.; Akiba, K.-Y. *Acta Crystallogr., Sect. C* **1987**, *C43*, 2338. (b) Ghosh, R.; Simonsen, S. H. *Acta Crystallogr., Sect. C* **1993**, *C49*, 1031. (c) Ackers, B.; Blake, A. J.; Hill, S. J.; Hubberstey, P. *Acta Crystallogr., Sect. C* **2002**, *C58*, o640. (d) Suzuki, T.; Fujii, H.; Yamashita, Y.; Kabuto, C.; Tanaka, S.; Harasawa, M.; Mukai, T.; Miyashi, T. *J. Am. Chem. Soc.* **1992**, *114*, 3034.
(20) (a) Hasenknopf, B.; Lehn, J.-M.; Kneisel, B. O.; Baum, G.; Fenske, D. *Angew. Chem., Int. Ed. Engl.* **1996**, *35*, 1838. (b) Plasseraud, L.; Maid, H.; Hampel, F.; Saalfrank, R. W. *Chem. Eur. J.* **2001**, *7*, 4007. (c) Slater, J. W.; Lydon, D. P.; Alcock, N. W.; Rourke, J. P. *Organometallics* **2001**, *20*, 4418.
(21) (a) Cuccia, L. A.; Ruiz, E.; Lehn, J.-M.; Homo, J.-C.; Schmutz, M. *Chem. Eur. J.* **2002**, *8*, 3448. (b) Cuccia, L. A.; Lehn, J.-M.; Homo, J.-C.; Schmutz, M. *Angew. Chem., Int. Ed.* **2000**, *39*, 233.
(22) (a) Bäuerle, P.; Pfau, F.; Schlupp, H.; Würthner, F.; Gaudl, K.-U.; Caro, M. B.; Fischer, P. *J. Chem. Soc., Perkin Trans. 2* **1993**, 489. (b) He, M.; Leslie, T. M.; Sinicropi, J. A. *Chem. Mater.* **2002**, *14*, 4662.

Table 1. Results of the Polymerization

no.	polymer	yield (%)	$M_n \times 10^{-4}$ [a]	$[\eta]$ (dL g^{-1})	T_d[e] (°C)
1	P(PydTh)-H	90	*b*	0.35[c]	391
2	P(PydTh)-6	93	9.0		407
3	P(PydTh)-10	95	16		415
4	P(PydTh)-12	94	16	0.89[d]	414
5	P(PydTh)-14	94	3.2		410

[a] Molecular weights were estimated from GPC analysis (eluent = 1,2-dichlorobenzene at 135 °C; polystyrene standards). [b] Not determined due to poor solubility. [c] In concentrated H_2SO_4 at 30 °C. [d] In 1,2-dichlorobenzene at 30 °C (for the soluble part (approximately 90%) of **P(PydTh)-12**). [e] 5% weight-loss temperature measured by TGA under N_2 with a heating rate of 10 °C min^{-1}.

FT-IR, and elemental analysis, and the data are provided in the Experimental Section.

According to the coupling reaction of **3a**−**3e** utilizing $Me_3Sn-SnMe_3$ as the condensing reagent and $Pd(PPh_3)_4$ and CuI as catalysts, the corresponding polymers were successfully obtained in high yields (90−95%). Recently, Chan and coworkers briefly reported a similar polymerization method using hexabutylditin ($Bu_3Sn-SnBu_3$),[23] based on the Stille−Kelly reaction.[24] We found that the utilization of $Me_3Sn-SnMe_3$ instead of $Bu_3Sn-SnBu_3$ and addition of CuI cocatalyst[25] accelerated the polymerization reaction and gave a higher molecular weight as described below. The Pd-catalyzed Suzuki-type polymerization using bis(pinacolato)-diboron,[26] instead of $R_3Sn-SnR_3$, was not effective for the monomers. π-Conjugated polymer with the pyridazine unit has no precedent to our knowledge.

The polymers, **P(PydTh)-6** through **P(PydTh)-14**, were partly (ca. 50−90%) soluble in organic solvents such as $CHCl_3$, THF, toluene, and 1,2-dichlorobenzene at room temperature. The main part (more than 90%) of the alkyl-substituted polymers was soluble in 1,2-dichlorobenzene at 135 °C; the solubility at the temperature was 10 mg/mL or higher. The gel permeation chromatography (GPC) analysis was carried out with the main part and using 1,2-dichlorobenzene as the eluent. The nonsubstituted **P(PydTh)-H** was almost insoluble in the aforementioned solvents and only partially soluble in HCOOH, CF_3COOH, and concentrated H_2SO_4. As shown in Table 1, the number-average molecular weights (M_ns) of the polymers with the alkyl side chain were estimated at $3.2-16 \times 10^4$ (for the 1,2-dichlorobenzene-soluble fraction vs polystyrene standards). The GPC traces exhibited considerably broad distribution of the molecular weight, and the GPC trace became bimodal for **P(PydTh)-6** through **P(PydTh)-12** (cf. Figure S1). Organometallic polycondensation sometimes gives a broad distribution of the molecular weight (e.g., an M_w/M_n value of 3.3[27a]). One of the reasons for the bimodal distribution is ascribed to occurrence of both reductive elimination and protonolysis

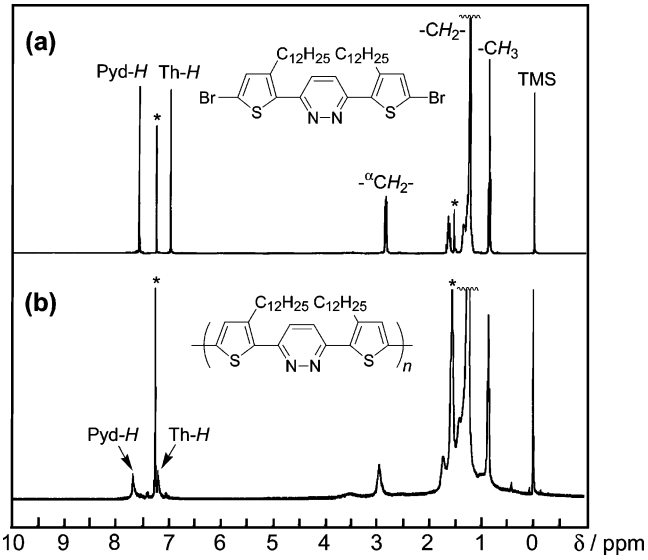

Figure 1. ^{1}H NMR spectra of (a) **3d** and (b) **P(PydTh)-12** in $CDCl_3$. The peaks with an asterisk mark are due to $CHCl_3$ and H_2O.

of organometallic species during workup.[27b,c] Aggregation of the polymer molecules even in fluid solution may also cause broadening of the GPC trace in the high molecular weight region.

The intrinsic viscosities $[\eta]$ of **P(PydTh)-H** (in concentrated H_2SO_4 at 30 °C) and the 1,2-dichlorobenzene-soluble part (ca. 90%) of **P(PydTh)-12** (in 1,2-dichlorobenzene at 30 °C) were 0.35 and 0.89 dL g^{-1}, respectively. The $[\eta]$ value of **P(PydTh)-12** corresponds to a molecular weight of 27×10^4 of polystyrene.[27d] **P(PydTh)-12** prepared with $Bu_3Sn-SnBu_3$ showed a lower molecular weight (M_n = 4100 vs polystyrene standards) and a narrow molecular weight distribution (M_w/M_n = 1.5) in the GPC analysis.

All the copolymers exhibited good thermal stability with 5% weight-loss temperatures (T_d) higher than 390 °C under N_2, as revealed by thermogravimetric analysis (TGA). The first weight-loss took place in the temperature range of 380−500 °C (cf. Figure S2).

NMR and IR. Figure 1 depicts ^{1}H NMR spectra of **3d** and **P(PydTh)-12** in $CDCl_3$. **P(PydTh)-12** shows two aromatic signals at δ 7.68 and 7.20, which are assigned to pyridazine-*H* and thiophene-*H*, respectively. The peaks in the range of δ 3.0−0.8 arise from alkyl groups, and the peak area ratio between the aromatic and aliphatic signals agrees with the molecular structure of **P(PydTh)-12**. **P(PydTh)-H** was characterized by cross-polarization magic-angle spinning (CP-MAS) ^{13}C NMR spectroscopy in the solid state, which is depicted in Figure S3; the *C*═N peak (δ 149) of the polymer appears near the *C*═N peak position (δ 148) of the monomer **3a**.

IR spectra of the polymers exhibited characteristic absorption peaks at about 1440 cm^{-1} (ring stretching vibration) and 830 cm^{-1} (C−H out-of-plane vibration) due to α,α′-coupled thiophene rings. The presence of a ν(C═N) peak at 1550

(23) Xu, J.; Ng, S. C.; Chan, H. S. O. *Tetrahedron Lett.* **2001**, *42*, 5327.
(24) (a) Stille, J. K.; *Angew. Chem., Int. Ed. Engl.* **1986**, *25*, 508. (b) Kelly, T. R.; Li, Q.; Bhushan, V. *Tetrahedron Lett.* **1990**, *31*, 161. (c) Fukuyama, Y.; Yaso, H.; Nakamura, K.; Kodama, M. *Tetrahedron Lett.* **1999**, *40*, 105.
(25) The beneficial effects of added CuI to the transmetalation step have been reported. See: (a) Bao, Z.; Chan, W. K.; Yu, L. *J. Am. Chem. Soc.* **1995**, *117*, 12426. (b) Saa, J. M.; Martorell, G. *J. Org. Chem.* **1993**, *58*, 1963. (c) Farina, V.; Kapadia, S.; Krishnan, B.; Wang, C.; Liebeskind, L. S. *J. Org. Chem.* **1994**, *59*, 5905.
(26) (a) Izumi, A.; Nomura, R.; Masuda, T. *Chem. Lett.* **2000**, 29, 728. (b) Izumi, A.; Nomura, R.; Masuda, T. *Macromolecules* **2000**, *33*, 8918.
(27) (a) Suh, H.; Jin, Y.; Park, S. H.; Kim, D.; Kim, J.; Kim, C.; Kim, J. Y.; Lee, K. *Macromolecules* **2005**, *38*, 6285. (b) Miyakoshi, R.; Yokoyama, Y.; Yokozawa, T. *Macromol. Rapid Commun.* **2004**, *25*, 1663. (c) Yamamoto, T.; Abla, M.; Murakami, Y. *Bull. Chem. Soc. Jpn.* **2002**, *75*, 1997. (d) McCormick, H. W. *J. Polym. Sci.* **1959**, *36*, 341.

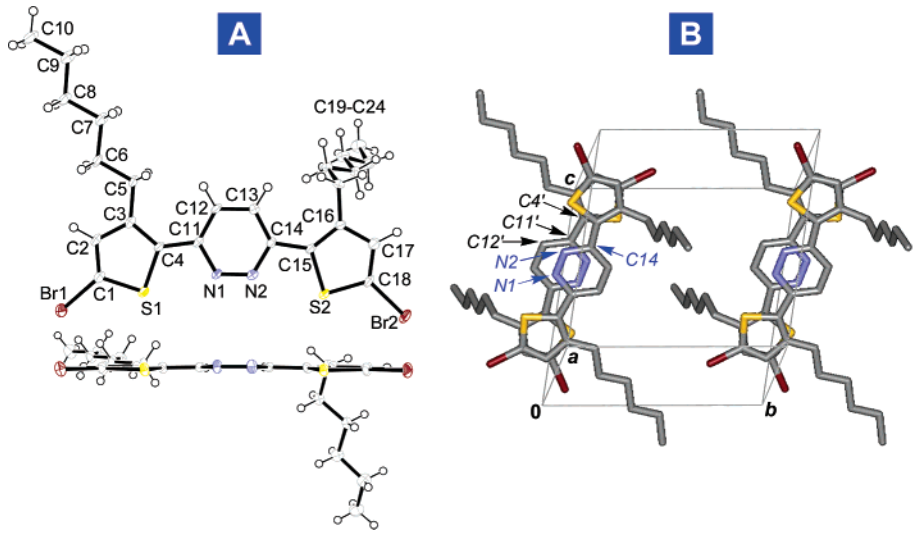

Figure 2. (A) ORTEP drawing (50% ellipsoids) of **3b**. Selected bond lengths (Å) and angles (deg): N1−N2 1.308(5), N1−C11 1.354(4), C11−C12 1.383(5), C12−C13 1.387(6), C4−C11 1.454(5), S1−C4 1.7343(4), S1−C1 1.716(4), C1−C2 1.358(5), C2−C3 1.417(6), C1−Br1 1.869(4), N2−N1−C11 121.2(3), N1−C11−C12 121.0(3), C11−C12−C13 118.2(3), N1−C11−C4 113.0(3), C12−C11−C4 126.0(3), N2−C14−C15 112.5(3), C13−C14−C15 126.2(3), N1−C11−C4−S1 2.5(4), N2−C14−C15−S2 2.7(4). (B) Crystal packing diagram of **3b**. Hydrogen atoms are omitted for clarity.

cm^{-1}, characteristic of the pyridazine unit, supports the notion that the pyridazine ring is maintained after the polymerization[28] (cf. Figure S4).

X-ray Structural Analysis of the Monomer. The X-ray crystal structure of **3b** was resolved. Figure 2 displays the ORTEP drawing and the crystal packing diagram of **3b**; the detailed crystallographic data are given in the Supporting Information.

The three aromatic rings of **3b** assume a highly coplanar structure with dihedral angles between the central pyridazine and the peripheral thiophene rings of less than 3°; consequently the steric hindrance between the thiophene-alkyl groups and the CH hydrogen atoms attached at the C12 and C13 carbons of the pyridazine ring is considered to be negligible. As apparently seen in Figure 2A, the two outer thiophene rings of **3b** bend toward the direction of nitrogen in the pyridazine unit, presumably due to intramolecular nonbonded interaction[29] between the sulfur and nitrogen atoms.[19] Because of this bending, conceivable steric repulsion between the thiophene-alkyl group and the pyridazine CH hydrogen is avoided. The intramolecular S1···N1 and S2···N2 distances of 2.78 and 2.76 Å, respectively, are significantly shorter than the sum of the corresponding van der Waals radii (3.35 Å)[30] and support the presence of the attractive nonbonded interaction, which stabilizes the coplanar conformation of **3b**. DFT[31a] theoretical calculations (B3LYP/6-31G* level)[31b−d] indicated a coplanar minimum-energy structure for a trimeric model compound, 3,6-bis[2-(3-ethylthienyl)]pyridazine (see Figure S5); the structure resembles the X-ray crystal structure of **3b**. When the trimeric units are connected (or polymerized) to form **P(PydTh)s**, there seems to be no apparent steric repulsion between the connecting two alkylthiophene units, if the two thiophene units assume an s-trans conformation. Consequently **P(PydTh)s** are considered to have an essentially coplanar structure.

As can be seen in Figure 2B, the crystal packing of **3b** is comprised of infinite π-stacks along the *a* lattice direction, in which the molecules are alternately arranged in an antiparallel fashion in view of the orientation of the central pyridazine unit. The short intermolecular contact distances, N1−C12′ (3.48 Å), N2−C11′ (3.47 Å), and C14−C4′ (3.47 Å), suggest strong intermolecular interactions between the stacked molecules. The face-to-face packing distance was roughly estimated at 3.4 Å. The antiparallel dipole−dipole interaction between facing polar pyridazine rings is considered to be a dominant factor to dictate the packing of molecules.[32] In the crystal, one hexyl group lies in the plane of the backbone, while the other one is kinked substantially out of the molecular plane to occupy a space between the packed molecules.

Self-Organized Solid Structure of the Polymers. Figure 3 displays the powder X-ray diffraction (XRD) patterns of the **P(PydTh)s**. The polymers with long alkyl side chains (charts b−e of Figure 3) exhibit sharp reflection peaks in the low-angle region, similar to HT-P3RTh.[2−5] For **P(PydTh)-14** (chart e of Figure 3), a distinct peak at 22.8 Å, indexed as a (100) reflection, will be assigned to the interchain spacing between the two polymer main chains, which is segregated by the alkyl substituents.[2−5] Its second-, third-, and forth-order reflections are clearly observed at 11.4, 7.6, and 5.7 (22.8/*n*; $n = 2-4$) Å, respectively, implying a highly ordered assembly of the polymer molecules. The

(28) For **P(PydTh)s**, the ν(C=N) peak appeared at somewhat lower frequency by about 40 cm^{-1} compared with that of 3,6-bis(2-pyridyl)-pyridazine. See: Hoogenboom, R.; Wouters, D.; Schubert, U. S. *Macromolecules* **2003**, *36*, 4743.

(29) (a) Iwaoka, M.; Takemoto, S.; Okada, M.; Tomoda, S. *Bull. Chem. Soc. Jpn.* **2002**, *75*, 1611. (b) Nagao, Y.; Hirata, T.; Goto, S.; Sano, S.; Kakehi, A.; Iizuka, K.; Shiro, M. *J. Am. Chem. Soc.* **1998**, *120*, 3104.

(30) Bondi, A. *J. Phys. Chem.* **1964**, *68*, 441.

(31) (a) Parr, R. G.; Yang, W. *Density-Functional Theory of Atoms and Molecules*; Oxford University Press: New York, 1989. (b) Becke, A. D. *J. Chem. Phys.* **1993**, *98*, 5648. (c) Lee, C.; Yang, W.; Parr, R. G. *Phys. Rev. B* **1988**, *37*, 785. (d) Hariharan, P. C.; Pople, J. A. *Chem. Phys. Lett.* **1972**, *16*, 217.

(32) Yasuda, T.; Imase, T.; Nakamura, Y.; Yamamoto, T. *Macromolecules* **2005**, *38*, 4687.

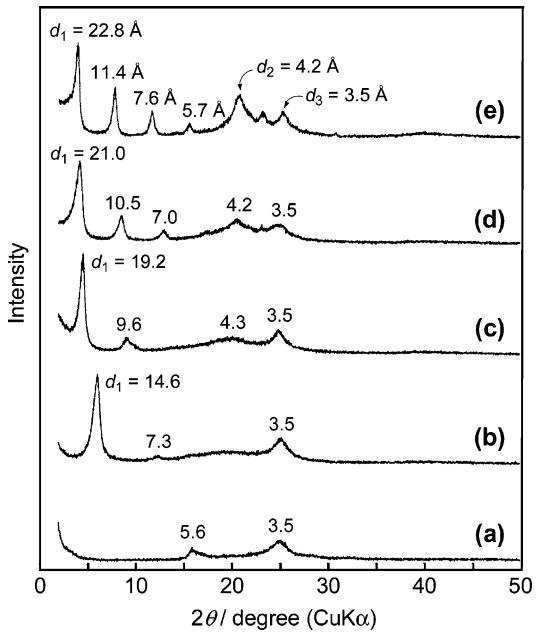

Figure 3. Powder X-ray diffractograms of (a) **P(PydTh)-H**, (b) **P(PydTh)-6**, (c) **P(PydTh)-10**, (d) **P(PydTh)-12**, and (e) **P(PydTh)-14**. Peaks are labeled with *d* spacing in angstroms.

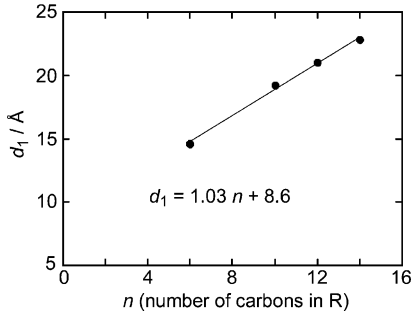

Figure 4. Plots of the d_1 spacing against the number of carbons (n) in the alkyl side chain for **P(PydTh)s**.

peaks of $d_2 = 4.2$ Å and $d_3 = 3.5$ Å are considered to originate from crystallization of the alkyl side chains and π-stacking of the coplanar polymer main chains (i.e., (010) reflection), respectively.[2−4,9a,33] The face-to-face π-stacked distance (d_3) of 3.5 Å observed with **P(PydTh)s** is almost the same as the intermolecular distance (ca. 3.4 Å) seen in the crystal structure of **3b** (cf. Figure 2B).

As shown in Figure 3, the interchain d_1 spacing reasonably increases upon elongation of the side chain from hexyl group (for **P(PydTh)-6**: $d_1 = 14.6$ Å) to tetradecyl group (for **P(PydTh)-14**: $d_1 = 22.8$ Å). Plots of the d_1 spacing against the number of carbons in the alkyl side chain give a linear line with a slope of 1.03 Å/carbon (see Figure 4), which is smaller than the height of one $-CH_2-$ unit (1.25 Å/carbon).[4,34] **P(PydTh)s** are presumed to adopt an interdigitation packing structure, because the number density of the alkyl groups is not as high as HT-P3RTh and the nonsubstituted pyridazine ring provides a sufficient space to facilitate the side-chain interdigitation, as illustrated in Figure 5. In the

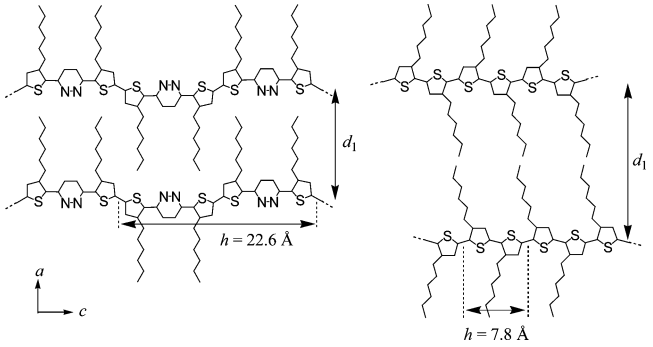

Figure 5. Schematic representation of arrangements of two polymer chains for **P(PydTh)s** (left) and HT-P3RTh (right).

Chart 2. Proposed Packing Structure of P(PydTh)-H

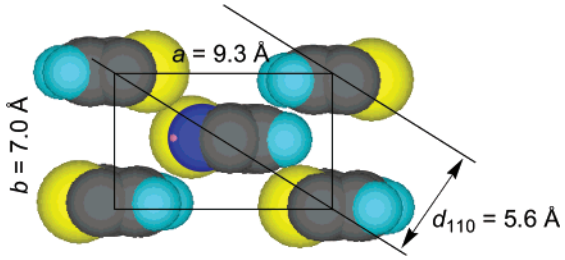

case of widely investigated HT-P3RTh, its high number density of the alkyl side chain (one alkyl chain/repeating height of 7.8 Å for a *trans*-bithiophene unit)[2,3] prevented formation of the interdigitation packing because of a rather large effective diameter ($d = 4.5$ Å)[34] of the alkyl side chain; consequently HT-P3RTh assumes an end-to-end packing mode.[2−4] On the contrary, the number density of the alkyl side chain for **P(PydTh)s** (4/22.6 Å or 1/5.65 Å) is smaller enough for the interdigitation packing. The alkyl side chains are considered to be somewhat tilted to fill out the allotted space effectively. The observed slope of 1.03 Å/carbon (Figure 4) less than the height of the $-CH_2-$ unit (1.25 Å/carbon) agrees with this view. In the packing structure, the alkyl chains in the upper layer are considered to be situated between those in the lower layer to attain a well-packed hexagonal-like packing structure. Similar XRD patterns, self-assembly, and packing models have been reported for one of the $(ABA)_n$-type copolymers (B = thiophene-2,5-diyl).[11a,16]

The packing model depicted in Figure 5 gave calculated densities[35] of 1.22, 1.16, 1.19, and 1.19 g cm^{-3} for **P(PydTh)-6** through **P(PydTh)-14**, respectively. These calculated values agreed well with observed densities of 1.22, 1.17, 1.15, and 1.14 g cm^{-3}, respectively, within the experimental error.

On the other hand, the XRD profile of **P(PydTh)-H** (Figure 3a) is simple and somewhat differs from those of the alkyl analogues. These features suggest a face-centered packing with the lateral unit cell dimensions of $a = 9.3$ Å and $b = 7.0$ Å, in which the molecular plane of **P(PydTh)-H** is in parallel to the *ac* plane (the *c* axis in the direction of polymer backbone). The dimensions of *a* and *b* are reason-

(33) Watanabe, J.; Harkness, B. R.; Sone, M.; Ichimura, H. *Macromolecules* **1994**, *27*, 507.
(34) (a) Jordan, E. F., Jr.; Feldeisen, D. W.; Wrigley, A. N. *J. Polym. Sci.: Part A* **1971**, *9*, 1835. (b) Hsieh, H. W. S.; Post, B.; Morawetz, H. *J. Polym. Sci.: Polym. Phys. Ed.* **1976**, *14*, 1241.

(35) Calculated density (g cm^{-3}) = $[(C_{12}H_4N_2S_2R_2{\cdot}xH_2O)/6.02 \times 10^{23}]/(11.3 \times 3.5 \times d_1 \times 10^{-24})$, where 11.3 Å and 3.5 Å are the lengths of the repeating height (h/2 in Figure 5) and the interlayer distance obtained from the XRD data, respectively.

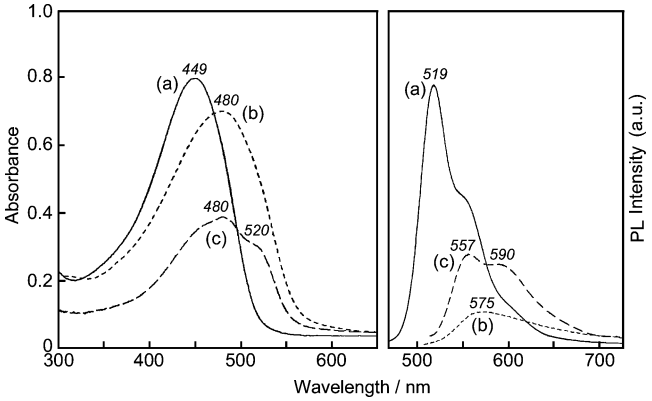

Figure 6. UV−vis absorption (left) and PL (right) spectra of **P(PydTh)-12** in (a) $CHCl_3$ (solid line), (b) HCOOH (short-dashed line), and (c) thin film (long-dashed line) at room temperature.

Chart 3. Comparison of UV−Vis Data of Thiophene-Based (ABA)$_n$-Type Copolymers

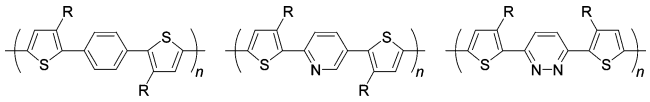

λ_{max} = 398 nm[14a] in $CHCl_3$, Φ = 19-26%

λ_{max} = 429-432 nm[14b] in $CHCl_3$, Φ = 40-44%

λ_{max} = 439-449 nm in $CHCl_3$, Φ = 51-61%

able for **P(PydTh)-H**, and the two major peaks at 5.6 Å and 3.5 Å can be indexed as (110) and (020) reflections, respectively (cf. Chart 2). When R of HT-P3RTh is shortened to methyl, the polymer takes a similar face-centered packing structure.[4,36]

For thin films of the polymers cast on a Pt plate, the XRD patterns clearly showed the d_1 peak; however, the d_2 and d_3 peaks became obscure (cf. Figure S6). These results suggest that the polymer molecules assume an aligned structure in the film, with the alkyl side chains oriented toward the surface of substrate. Recently similar alignment of π-conjugated polymers, including the (ABA)$_n$-type polymers[11a] with alkyl side chains, on the surface of substrates has been reported.[5c,9c,32]

UV−Vis Absorption and Photoluminescence (PL). Figure 6 depicts the UV−vis absorption and PL spectra of **P(PydTh)-12** in solutions and film. The absorption peak (λ_{max}) at 449 nm in $CHCl_3$ (curve a of Figure 6) is considered to be due to the $\pi-\pi^*$ transition along the polymer main chain, which takes place at a lower energy than those of similar thiophene-based (ABA)$_n$-type copolymers possessing *p*-phenylene[14a] or pyridine-2,5-diyl[14b] central unit (see Chart 3). This bathochromic shift of the absorption peak may be related to an enhanced CT electronic structure of the polymer[7a,9a,32] and/or high coplanarity of **P(PydTh)-12**. **P(PydTh)-12** exhibits strong-green PL with the emission maximum (λ_{em}) at 519 nm in $CHCl_3$, which essentially agrees with the onset position of the absorption band, as usually observed with aromatic compounds and polymers. The PL quantum yield of **P(PydTh)-12** (Φ = 58% in $CHCl_3$) is higher than those of similar copolymers[14a,b] shown in Chart 3 and P3RTh (Φ = 11% in $CHCl_3$).[37]

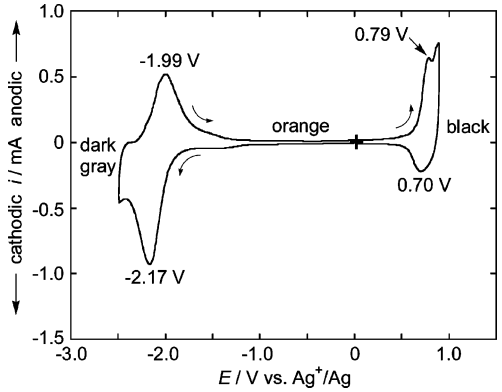

Figure 7. Cyclic voltammogram of a film of **P(PydTh)-12** on a Pt plate in an acetonitrile solution of $[(C_2H_5)_4N]BF_4$ (0.10 M) under N_2. Scan rate is 50 mV s^{-1}.

The λ_{max} of the thin film (curve c in Figure 6) was red-shifted by approximately 30 nm from that in $CHCl_3$, and an additional shoulder peak was observed at 520 nm. Such a bathochromic shift of the λ_{max} position in going from the solution to the solid state is often observed with π-conjugated polymers and is indicative of aggregation, which leads to an intermolecular $\pi-\pi$ electronic interaction in the stacked polymers and/or planarization of the backbone conformation. Because **P(PydTh)-12** is considered to assume a coplanar structure even in the solution, the bathochromic shift is mainly accounted for by the intermolecular electronic interaction. **P(PydTh)-12** prepared by using $Bu_3Sn-SnBu_3$ and having the lower molecular weight showed the UV−vis peak at somewhat shorter wavelength (440 nm in $CHCl_3$ and 467 nm in film).

The PL spectrum (curve c in Figure 6) also showed a shift to a longer wavelength in film. Although PL of many π-conjugated polymers such as HT-P3RTh is strongly weakened in the solid state, especially when they form such a π-stacked structure, the film of **P(PydTh)-12** exhibited considerably strong PL.

P(PydTh)-12 showed a conspicuous red-shift of UV−vis and PL peaks in HCOOH (curve b in Figure 6), revealing a strong effect for the protonation of the nitrogens of the pyridazine unit on the optical properties. The PL emission from **P(PydTh)-12** was significantly weakened (Φ < 1%). These phenomena in the acidic medium would be related to enhancement of the intramolecular CT from the electron-donating thiophene unit to the electron-accepting pyridazine unit by the protonation.[38] A similar solvatochromic effect has been observed in the protonation of π-conjugated copolymers containing 1,10-phenanthroline or pyridine unit.[39]

Electrochemical Redox Behavior. A typical cyclic voltammogram of a cast film is depicted in Figure 7 for **P(PydTh)-12**. Since **P(PydTh)-12** contains both electron-accepting pyridazine and electron-donating thiophene units, the polymer film accepts both electrochemical n-doping and p-doping. The electrochemical reduction of **P(PydTh)-12** starts at about −1.8 V with an n-doping peak at −2.17 V vs Ag^+/Ag, and the corresponding oxidation (n-dedoping) peak appears at −1.99 V vs Ag^+/Ag.

(36) Yamamoto, T.; Lee, B.-L.; Suganuma, H.; Sasaki, S. *Polym. J.* **1998**, *30*, 853.
(37) Li, L.; Collard, D. M. *Macromolecules* **2005**, *38*, 372.
(38) Valeur, B.; Leray, I. *Coord. Chem. Rev.* **2000**, *205*, 3.
(39) Yasuda, T.; Yamamoto, T. *Macromolecules* **2003**, *36*, 7513.

Table 2. Optical and Electrochemical Data of the Polymers

		UV−vis absorption λ_{max} (nm)			PL λ_{em} (nm)			redox peak potential[g] (V vs Ag^+/Ag)		
no.	polymer	solution[a]	film[c]	E_g^{opte} (eV)	solution[a]	film[c]	Φ^f (%)	n-doping	p-doping	E_g^{ele} [i] (eV)
1	P(PydTh)-H	474[b]	*d*	*d*	553[b]	*d*	<1[b]	−2.15	1.18[h]	2.47
2	P(PydTh)-6	449	472 (516)	2.21	517 (553)	561 (597)	61	−2.18	0.80	2.34
3	P(PydTh)-10	448	480 (516)	2.22	519 (555)	557 (592)	59	−2.18	0.76	2.42
4	P(PydTh)-12	449	480 (515)	2.22	519 (554)	557 (590)	58	−2.17	0.79	2.38
5	P(PydTh)-14	439	464 (510)	2.25	513 (548)	555 (587)	51	−2.28	0.85	2.50

[a] With the $CHCl_3$ soluble part and in $CHCl_3$, unless otherwise noted. [b] Measured in HCOOH. [c] Thin polymer film cast on a quartz glass plate. The data in parentheses are due to shoulder peaks. [d] Not determined. [e] Band-gap energy estimated from the onset position of UV−vis spectra in film. [f] PL quantum yield in $CHCl_3$ calculated using the standard of quinine sulfate (10^{-5} M solution in 0.5 M H_2SO_4) having Φ of 54.6%. [g] Measured by cyclic voltammetry for the film on a Pt plate in an acetonitrile solution of $[(C_2H_5)_4N]BF_4$. [h] Irreversible wave. [i] Band gap energy estimated from the onset reduction and onset oxidation potentials in cyclic voltammetry.

The p-doping and p-dedoping redox peaks are observed at normal positions (0.79 and 0.70 V vs Ag^+/Ag, respectively) for thiophene-based polymers. A large potential difference between the p-doping and p-dedoping was previously reported for the copolymer of thiophene and pyridine (PThPy shown in the Introduction part).[7a] In the previously reported case, the polymer molecules assume a twisted conformation, and the electrochemical oxidation may bring about a relatively large structural relaxation, leading such a potential discrepancy. However, for **P(PydTh)-12**, such a large potential difference was not observed between the p-doping and p-dedoping.

The cyclic voltammogram of **P(PydTh)-12** was stable and reproducible through repeated scannings. However, the polymer was sensitive to overoxidation,[40] and scanning to a higher potential (higher than 1.3 V vs Ag^+/Ag) resulted in the destruction of the electrochemical activity of the polymer. The electrochemical data for the polymers are presented in Table 2. In the case of **P(PydTh)-H**, the p-doping potential shifted to a higher potential by about 400 mV from that of the alkyl analogues; the data are consistent with an electron-donating nature of the alkyl substituent.

The lowest-unoccupied molecular orbital (LUMO) and the highest-occupied molecular orbital (HOMO) energy levels (E_{LUMO} and E_{HOMO}) of the copolymers were deduced as −3.0 to −2.8 eV and −5.5 to −5.2 eV, respectively, from the onset potentials of n- and p-doping waves in the cyclic voltammograms.[41] Accordingly, the electrochemically evaluated band gap, E_g^{ele} ($E_{LUMO} - E_{HOMO}$), ranges from 2.3 to 2.5 eV, as indicated in Table 2.

Electrochromic Behavior. To study spectroelectrochemical behavior of **P(PydTh)-12**, a cast film was prepared on an indium−tin−oxide (ITO) coated glass substrate. Figure 8 presents the UV−vis−NIR absorption spectra of **P(PydTh)-12** at various applied potentials between −2.4 and +1.0 V vs Ag^+/Ag. When the applied potential was negatively increased from 0 to −2.4 V (Figure 8, top), intensity of the $\pi-\pi^*$ absorption band at about 480 nm in the neutral polymer decreased. This electrochemical reduction brought about a new broad absorption band centered around 850 nm and tailing into the NIR region, which may have originated from polaronic states. By returning to 0 V vs Ag^+/Ag, the original UV−vis spectrum was recovered. These spectroscopic changes along the n-doping/n-dedoping processes were recognized as a color change between orange and dark-gray. This electrochromism showed good reversibility and fast response (cf. Figure S7).

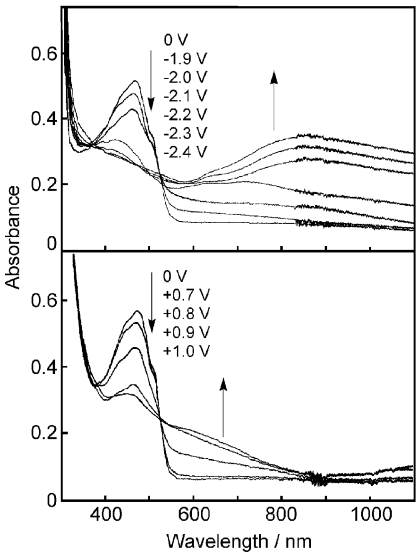

Figure 8. Changes in the absorption spectrum of a film of **P(PydTh)-12** on an ITO glass plate during the electrochemical n-doping (top) and p-doping (bottom) in an acetonitrile solution of $[(C_2H_5)_4N]BF_4$ (0.10 M). Arrows indicate the direction of the spectral change.

Upon application of the oxidative potentials (Figure 8, bottom), the $\pi-\pi^*$ absorption band of **P(PydTh)-12** became weaker, and a broad absorption emerged in the range of 600−800 nm.

Field-Effect Transistor Characteristics. Thin-film field-effect transistors (FETs) using **P(PydTh)-6** as the semiconductor layer were fabricated on n-doped Si/SiO_2 substrates by spin-coating (see the Supporting Information). The device structure is shown in Figure 9A. Figure 9B displays the plots of source-drain current (I_{DS}) as a function of source-drain voltage (V_{DS}) at different gate voltage (V_G) from 0 to −60 V. On the application of negative V_G, characteristic transistor behavior was observed, indicating that the fabricated FET had p-channel characteristics. However, we could not obtain n-channel characteristics for the device, possibly due to a large barrier for electron injection from the Au electrode into the polymer.

As the V_{DS} increases, the current I_{DS} enters into the saturation regime and can be described by the following

(40) Krische, B.; Zagorska, M. *Synth. Met.* **1989**, *28*, 257.

(41) All electrochemical onset potentials were calibrated with the Fc^+/Fc standard (4.8 eV below the vacuum level) to estimate the LUMO and HOMO energy levels of the polymers. See: (a) Pommerehne, J.; Vestweber, H.; Guss, W.; Mahrt, R. F.; Bässler, H.; Porsch, M.; Daub, J. *Adv. Mater.* **1995**, *7*, 551. (b) Liu, M. S.; Jiang, X.; Liu, S.; Herguth, P.; Jen, A. K.-Y. *Macromolecules* **2002**, *35*, 3532.

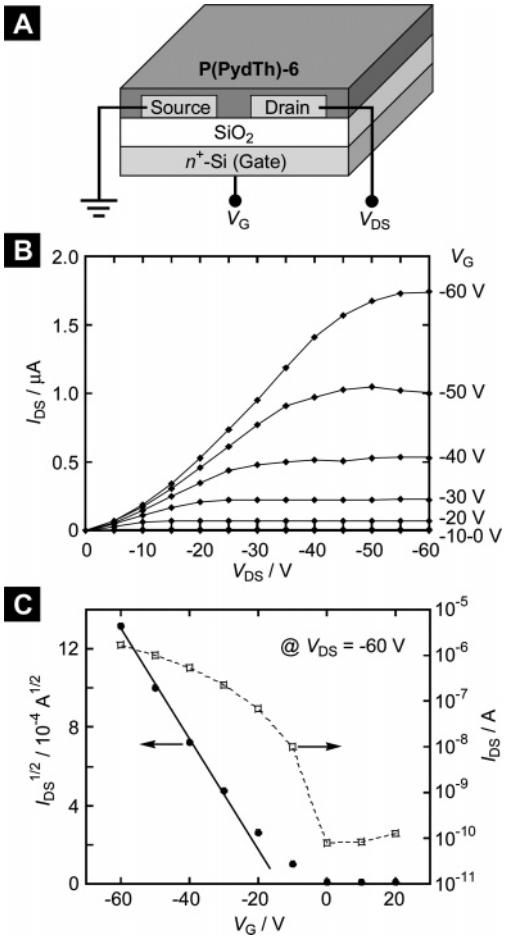

Figure 9. (A) Schematic illustration of the bottom-contact field-effect transistor (FET) based on **P(PydTh)-6**. The source and drain electrodes consist of Au contact. (B) Source-drain current (I_{DS}) vs source-drain voltage (V_{DS}) output characteristics of the device. (C) Transfer characteristics of the same device taken at $V_{DS} = -60$ V.

equation

$$I_{DS} = \frac{WC_i}{2L}\mu(V_G - V_T)^2 \qquad (1)$$

Here, W is the channel width (500 μm), L is the channel length (10 μm), μ is the field-effect carrier mobility, C_i is the capacitance per unit area of the insulation layer (11.5 nFcm^{-2}), and V_T is the threshold voltage. According to eq 1, μ was calculated to be 3×10^{-3} cm^2 V^{-1} s^{-1} from the linear portion of the transfer plots at a fixed V_{DS} of -60 V (see Figure 9C). The corresponding on/off current ratio of the device was evaluated as 4×10^3.

Conclusions

New donor−acceptor arranged π-conjugated copolymers, poly{3,6-bis[2-(3-alkylthienyl)]pyridazine}s (**P(PydTh)s**), were prepared via the elaborated polycondensation utilizing hexamethylditin. The pyridazine unit is a new building block for π-conjugated polymers. The polymers having long alkyl groups were soluble in organic solvents, and the solutions exhibited strong PL with the quantum yield higher than 50%. Single-crystal X-ray crystallography of the monomer and powder XRD of the polymer indicated that the polymers took a coplanar molecular structure and formed a supramolecular π-stacked assembly in the solid state. The UV−vis peak of the polymers shifted to a longer wavelength in film, indicating the occurrence of intermolecular electronic interactions; however, the polymer was still photoluminescent in the film. The PL was sensitive to the protonation. The electrochemical responses of the polymers in both the p- and n-doping processes were revealed, and the polymer showed good response in electrochromism even in the reductive region. The polymer demonstrated a carrier mobility of 3×10^{-3} cm^2 V^{-1} s^{-1} when used as a p-type semiconductor in the field-effect transistor.

Experimental Section

Synthetic Procedures. 3,6-Bis(2-thienyl)pyridazine (2a). To a stirred suspension of magnesium turnings (2.67 g, 110 mmol) in dry THF (50 mL) was slowly added **1a** (17.12 g, 105 mmol) under N_2. Thereafter, the mixture was stirred for 8 h at 60 °C. The produced Grignard reagent was transferred into a mixture of 3,6-dichloropyridazine (7.45 g, 50 mmol) and $NiCl_2$(dppp) (0.54 g, 1.0 mmol) in dry THF (50 mL) at 0 °C. The mixture was warmed to 60 °C and stirred for 17 h. After cooling, the reaction mixture was poured into a large amount of water, and the product was extracted with chloroform. The organic layer was washed with water and dried over anhydrous sodium sulfate. After filtration and evaporation, the crude product was washed with methanol and recrystallized from chloroform/hexane to afford a pale-yellow solid of **2a** (yield = 7.06 g, 58%). ^{1}H NMR (400 MHz, $CDCl_3$): δ 7.74 (s, 2H), 7.65 (dd, J = 4.0 and 1.2 Hz, 2H), 7.48 (dd, J = 4.8 and 1.2 Hz, 2H), 7.15 (dd, J = 4.8 and 4.0 Hz, 2H). ^{13}C{^{1}H} NMR (100 MHz, $CDCl_3$): δ 153.23, 140.61, 129.10, 127.99, 125.88, 122.42. Anal. Calcd for $C_{12}H_8N_2S_2$: C, 58.99; H, 3.30; N, 11.47; S, 26.25. Found: C, 59.18; H, 3.30; N, 11.43; S, 25.99.

2b−**2e** were prepared in a similar manner, and the product was purified by column chromatography (silica, chloroform/hexane = 2:1, v/v). Spectroscopic and analytical data of **2b**−**2e** are shown below.

3,6-Bis[2-(3-*n*-hexylthienyl)]pyridazine (2b). Yellow oil (yield = 74%). ^{1}H NMR (400 MHz, $CDCl_3$): δ 7.66 (s, 2H), 7.37 (d, J = 5.2 Hz, 2H), 7.03 (d, J = 5.2 Hz, 2H), 2.95 (t, J = 7.6 Hz, 4H), 1.68 (m, 4H), 1.38−1.28 (m, 12H), 0.87 (t, J = 7.2 Hz, 6H). ^{13}C-{^{1}H} NMR (100 MHz, $CDCl_3$): δ 153.80, 142.73, 133.60, 130.75, 126.89, 124.45, 31.70, 30.51, 29.76, 29.25, 22.64, 14.12. Anal. Calcd for $C_{24}H_{32}N_2S_2$: C, 69.85; H, 7.82; N, 6.79; S, 15.54. Found: C, 69.49; H, 7.65; N, 6.51; S, 15.20.

3,6-Bis[2-(3-*n*-decylthienyl)]pyridazine (2c). Light-yellow oil (yield = 59%). ^{1}H NMR (400 MHz, $CDCl_3$): δ 7.66 (s, 2H), 7.38 (d, J = 5.2 Hz, 2H), 7.03 (d, J = 5.2 Hz, 2H), 2.95 (t, J = 7.6 Hz, 4H), 1.69 (m, 4H), 1.38−1.24 (m, 28H), 0.87 (t, J = 6.8 Hz, 6H). ^{13}C{^{1}H} NMR (100 MHz, $CDCl_3$): δ 153.83, 142.76, 133.62, 130.77, 126.90, 124.47, 31.93, 30.57, 29.78, 29.66, 29.64, 29.62, 29.55, 29.38, 22.73, 14.18. Anal. Calcd for $C_{32}H_{48}N_2S_2$: C, 73.23; H, 9.22; N, 5.34; S, 12.22. Found: C, 72.96; H, 8.97; N, 5.15; S, 11.86.

3,6-Bis[2-(3-*n*-dodecylthienyl)]pyridazine (2d). Light-yellow solid (yield = 62%). ^{1}H NMR (400 MHz, $CDCl_3$): δ 7.66 (s, 2H), 7.38 (d, J = 5.2 Hz, 2H), 7.03 (d, J = 5.2 Hz, 2H), 2.96 (t, J = 7.6 Hz, 4H), 1.69 (m, 4H), 1.38−1.24 (m, 36H), 0.87 (t, J = 6.8 Hz, 6H). ^{13}C{^{1}H} NMR (100 MHz, $CDCl_3$): δ 153.86, 142.79, 133.65, 130.79, 126.90, 124.49, 31.97, 30.59, 29.80, 29.73, 29.71, 29.66, 29.62, 29.57, 29.40, 22.75, 14.18. Anal. Calcd for $C_{36}H_{56}N_2S_2$: C, 74.42; H, 9.72; N, 4.82; S, 11.04. Found: C, 74.58; H, 9.66; N, 4.68; S, 10.76.

3,6-Bis[2-(3-*n*-tetradecylthienyl)]pyridazine (2e). Light-yellow solid (yield = 60%). ^{1}H NMR (400 MHz, $CDCl_3$): δ 7.66 (s, 2H), 7.38 (d, J = 5.2 Hz, 2H), 7.03 (d, J = 5.2 Hz, 2H), 2.95 (t, J = 7.6

Hz, 4H), 1.69 (m, 4H), 1.38−1.24 (m, 36H), 0.88 (t, J = 6.8 Hz, 6H). $^{13}C\{^1H\}$ NMR (100 MHz, $CDCl_3$): δ 153.84, 142.77, 133.63, 130.78, 126.91, 124.48, 31.97, 30.58, 29.79, 29.74, 29.71, 29.66, 29.62, 29.57, 29.41, 22.75, 14.19. Anal. Calcd for $C_{40}H_{64}N_2S_2$: C, 75.41; H, 10.13; N, 4.40; S, 10.07. Found: C, 75.28; H, 10.19; N, 4.31; S, 9.83.

3,6-Bis[2-(5-bromothienyl)]pyridazine (3a). To a solution of **2a** (1.71 g, 7.0 mmol) in dry DMF (50 mL) was slowly added NBS (2.62 g, 14.7 mmol) at room temperature under N_2. The mixture was stirred for 12 h at 60 °C and then cooled to room temperature. The formed precipitate was separated by filtration, washed with water and methanol (twice), and dried under vacuum to give a light-yellow powder of **3a** (yield = 2.70 g, 96%). ^1H NMR (400 MHz, $CDCl_3$): δ 7.69 (s, 2H), 7.38 (d, J = 4.4 Hz, 2H), 7.11 (d, J = 4.4 Hz, 2H). CP-MAS ^{13}C NMR: δ 148.02, 137.75, 123.87, 118.99. FT-IR (KBr, cm^{-1}): 3091, 3061, 1579, 1552, 1435, 1401, 1325, 1216, 1121, 1061, 990, 856, 839, 792, 748. Anal. Calcd for $C_{12}H_6Br_2N_2S_2$: C, 35.84; H, 1.50; Br, 39.74; N, 6.97; S, 15.95. Found: C, 35.97; H, 1.56; Br, 39.48; N, 6.90; S, 15.72.

The synthesis of **3b**−**3e** was carried out analogously with the exception of the following workup and purification procedure. After the reaction, the resulting mixture was poured into a large amount of water, and the product was extracted with chloroform. The organic layer was washed with water and dried over anhydrous sodium sulfate. After filtration and evaporation, the product was purified by column chromatography (silica, chloroform/hexane = 1:1, v/v) and recrystallized from chloroform/methanol. Spectroscopic and analytical data of **3b**−**3e** are described below.

3,6-Bis[2-(5-bromo-3-*n*-hexylthienyl)]pyridazine (3b). Light-yellow solid (yield = 73%). ^1H NMR (400 MHz, $CDCl_3$): δ 7.59 (s, 2H), 6.98 (s, 2H), 2.86 (t, J = 7.6 Hz, 4H), 1.66 (m, 4H), 1.38−1.29 (m, 12H), 0.88 (t, J = 6.8 Hz, 6H). $^{13}C\{^1H\}$ NMR (100 MHz, $CDCl_3$): δ 153.04, 143.33, 135.25, 133.48, 123.92, 115.23, 31.67, 30.28, 29.84, 29.20, 22.62, 14.13. FT-IR (KBr, cm^{-1}): 2951, 2928, 2850, 1553, 1433, 1387, 1201, 1144, 1040, 1008, 823, 729. Anal. Calcd for $C_{24}H_{30}Br_2N_2S_2$: C, 50.53; H, 5.30; Br, 28.01; N, 4.91; S, 11.24. Found: C, 50.19; H, 5.31; Br, 28.34; N, 4.88; S, 11.10.

3,6-Bis[2-(5-bromo-3-*n*-decylthienyl)]pyridazine (3c). Light-yellow solid (yield = 72%). ^1H NMR (400 MHz, $CDCl_3$): δ 7.59 (s, 2H), 6.98 (s, 2H), 2.86 (t, J = 7.6 Hz, 4H), 1.65 (m, 4H), 1.37−1.25 (m, 28H), 0.87 (t, J = 6.8 Hz, 6H). $^{13}C\{^1H\}$ NMR (100 MHz, $CDCl_3$): δ 153.04, 143.33, 135.26, 133.48, 123.91, 115.22, 31.94, 30.32, 29.83, 29.65, 29.60, 29.52, 29.49, 29.37, 22.74, 14.19. FT-IR (KBr, cm^{-1}): 3048, 2954, 2918, 2850, 1550, 1469, 1439, 1390, 1121, 1042, 1006, 872, 827, 720. Anal. Calcd for $C_{32}H_{46}Br_2N_2S_2$: C, 56.30; H, 6.79; Br, 23.41; N, 4.10; S, 9.39. Found: C, 56.34; H, 6.57; Br, 23.77; N, 4.36; S, 9.32.

3,6-Bis[2-(5-bromo-3-*n*-dodecylthienyl)]pyridazine (3d). Light-yellow solid (yield = 88%). ^1H NMR (400 MHz, $CDCl_3$): δ 7.58 (s, 2H), 6.98 (s, 2H), 2.86 (t, J = 7.6 Hz, 4H), 1.66 (m, 4H), 1.37−1.25 (m, 36H), 0.88 (t, J = 6.8 Hz, 6H). $^{13}C\{^1H\}$ NMR (100 MHz, $CDCl_3$): δ 153.08, 143.38, 135.28, 133.51, 123.93, 115.21, 31.97, 30.33, 29.85, 29.72, 29.70, 29.60, 29.52, 29.50, 29.41, 22.75, 14.18. FT-IR (KBr, cm^{-1}): 3047, 2953, 2918, 2850, 1550, 1469, 1439, 1389, 1329, 1121, 1044, 1003, 871, 828, 720. Anal. Calcd for $C_{36}H_{54}Br_2N_2S_2$: C, 58.53; H, 7.37; Br, 21.63; N, 3.79; S, 8.68. Found: C, 58.26; H, 7.24; Br, 21.79; N, 3.84; S, 8.57.

3,6-Bis[2-(5-bromo-3-*n*-tetradecylthienyl)]pyridazine (3e). Light-yellow solid (yield = 75%). ^1H NMR (400 MHz, $CDCl_3$): δ 7.59 (s, 2H), 6.98 (s, 2H), 2.86 (t, J = 7.6 Hz, 4H), 1.37−1.25 (m, 44H), 0.88 (t, J = 6.8 Hz, 6H). $^{13}C\{^1H\}$ NMR (100 MHz, $CDCl_3$): δ 153.05, 143.35, 135.27, 133.49, 123.92, 115.23, 31.98, 30.32, 29.84, 29.76, 29.73, 29.71, 29.61, 29.52, 29.50, 29.42, 22.76, 14.20. FT-IR (KBr, cm^{-1}): 3047, 2953, 2918, 2849, 1551, 1468, 1439, 1391, 1330, 1122, 1044, 1004, 872, 827, 721. Anal. Calcd for $C_{40}H_{62}Br_2N_2S_2$: C, 60.44; H, 7.86; Br, 20.10; N, 3.52; S, 8.07. Found: C, 60.78; H, 7.87; Br, 20.19; N, 3.55; S, 8.35.

General Procedure for the Polymerization. Poly[3,6-bis(2-thienyl)pyridazine] (P(PydTh)-H). To a mixture of **3a** (1.21 g, 3.00 mmol) and hexamethylditin (1.03 g, 3.15 mmol) in dry THF (20 mL) and dry NMP (10 mL) were added $Pd(PPh_3)_4$ (0.17 g, 0.15 mmol) and copper(I) iodide (0.02 g, 0.1 mmol) as the catalysts. After being stirred for 48 h at 80 °C under N_2, the reaction mixture was added into an aqueous solution (ca. 5%) of potassium fluoride. The precipitated polymer was separated by filtration and then washed with distilled water, methanol, and acetone in this order. After drying under vacuum, red-brown powder of **P(PydTh)-H** was obtained (yield = 0.65 g, 90%). CP-MAS ^{13}C NMR: δ 148.60, 135.30, 122.51. FT-IR (KBr, cm^{-1}): 3064, 1549, 1438, 1405, 1311, 1119, 1075, 1036, 838, 793, 746, 696. Anal. Calcd for $(C_{12}H_6N_2S_2 \cdot 0.9H_2O)_n$: C, 55.75; H, 3.04; N, 10.84; S, 24.81. Found: C, 55.88; H, 2.76; N, 10.72; S, 24.29; Br, 3.50.

Other polymers were prepared in an analogous manner. The spectroscopic and analytical data of the polymers are described below.

Poly{3,6-bis[2-(3-*n*-hexylthienyl)]pyridazine} (P(PydTh)-6). Red powder (yield = 93%). ^1H NMR (400 MHz, $CDCl_3$): δ 7.69 (s, 2H), 7.21 (s, 2H), 2.97 (br, 4H), 1.74 (br, 4H), 1.45−1.34 (m, 12H), 0.91 (br, 6H). FT-IR (KBr, cm^{-1}): 2952, 2924, 2853, 1550, 1435, 1379, 1277, 1038, 826, 724. Anal. Calcd for $(C_{24}H_{30}N_2S_2 \cdot 0.8H_2O)_n$: C, 67.82; H, 7.49; N, 6.59; S, 15.09. Found: C, 67.54; H, 7.11; N, 6.34; S, 14.97; Br, 1.91.

Poly{3,6-bis[2-(3-*n*-decylthienyl)]pyridazine} (P(PydTh)-10). Red powder (yield = 95%). ^1H NMR (400 MHz, $CDCl_3$): δ 7.68 (s, 2H), 7.20 (s, 2H), 2.96 (br, 4H), 1.72 (br, 4H), 1.43−1.27 (m, 28H), 0.88 (br, 6H). FT-IR (KBr, cm^{-1}): 2922, 2851, 1550, 1436, 1380, 1272, 1038, 826, 720. Anal. Calcd for $(C_{32}H_{46}N_2S_2 \cdot 0.5H_2O)_n$: C, 72.26; H, 8.91; N, 5.27; S, 12.06. Found: C, 72.07; H, 8.49; N, 5.19; S, 11.80; Br, 0.36.

Poly{3,6-bis[2-(3-*n*-dodecylthienyl)]pyridazine} (P(PydTh)-12). Red powder (yield = 94%). ^1H NMR (400 MHz, $CDCl_3$): δ 7.68 (s, 2H), 7.20 (s, 2H), 2.95 (br, 4H), 1.74 (br, 4H), 1.44−1.25 (m, 36H), 0.87 (br, 6H). FT-IR (KBr, cm^{-1}): 2922, 2850, 1550, 1436, 1380, 1271, 1038, 826, 720. Anal. Calcd for $(C_{36}H_{54}N_2S_2 \cdot 0.8H_2O)_n$: C, 72.87; H, 9.44; N, 4.72; S, 11.00. Found: C, 72.79; H, 8.92; N, 4.65; S, 10.81; Br, 0.43.

Poly{3,6-bis[2-(3-*n*-tetradecylthienyl)]pyridazine} (P(PydTh)-14). Orange powder (yield = 94%). ^1H NMR (400 MHz, $CDCl_3$): δ 7.67 (s, 2H), 7.19 (s, 2H), 2.95 (br, 4H), 1.72 (br, 4H), 1.45−1.25 (m, 44H), 0.87 (br, 6H). FT-IR (KBr, cm^{-1}): 2920, 2850, 1550, 1466, 1438, 1382, 1274, 1038, 826, 721. Anal. Calcd for $(C_{40}H_{62}N_2S_2 \cdot 0.7H_2O)_n$: C, 74.12; H, 9.87; N, 4.33; S, 9.90. Found: C, 73.92; H, 9.25; N, 4.26; S, 9.88; Br, 0.

Instruments and Methods. Details for the measurements are given in the Supporting Information.

Acknowledgment. The authors are grateful to Dr. Y. Nakamura of our laboratory for his help in CP-MAS ^{13}C NMR measurements and Dr. T. Imase for his support in the quantum chemical calculations. This research was partly supported by a grant for the 21st Century Center of Excellence program.

Supporting Information Available: Spectroscopic data of **1b**−**1e**, table of X-ray crystal data of **3b**, GPC data, thermogravimetric analysis curves, NMR and FT-IR spectra, XRD data of the polymers, frontier orbital representation for the model compound (PDF), and crystallographic information file for **3b** (CIF). This material is available free of charge via the Internet at http://pubs.acs.org.

CM051561Y